Supporting Information

The Thermo-Responsive Behavior in Molecular Crystals of Naphthalene Diimides and Their 3D Printed Thermochromic Composites

Madushani Dharmarwardana, [a,†] Bhargav S. Arimilli,[a,†] Michael A. Luzuriaga,[a] Sunah Kwon,[b] Hamilton Lee,[a] Gayan A. Appuhamillage,[a] Gregory T. McCandless,[a] Ronald A. Smaldone,[a,*] Jeremiah J. Gassensmith[a,c,*]
[a]Department of Chemistry and Biochemistry, Department of Material Science and Engineering, [c]Department of Biomedical Engineering, University of Texas at Dallas, 800 West Campbell Road, Richardson, TX 75080-3021, USA.

[†]These authors contributed equally to this manuscript

*Corresponding Author: gassensmith@utdallas.edu, ronald.smaldone@utdallas.edu

Contents

Materials

Some of the chemicals and solvents used for synthesis and characterization (1,4,5,8-naphthalenetetracarboxylic dianhydride, 1-bromooctane, chloroform) were purchased from Sigma Aldrich. Others (1-bromobutane, 1-bromopentane, 1-bromoheptane, 1-bromooctane, 1-bromononane, 1-methyl-2-pyrrolidinone) were purchased from Alfa Aesar. Methylene chloride and acetone were purchased from Fischer Scientific.

Instrumentation

Nuclear Magnetic Resonance (NMR)

NMR spectra were measured using a Bruker ASCEND 600 MHz spectrometer in $CDCl_3$ and DMSO-d_6 using $Si(CH_3)_4$ as a reference standard.

ATR (attenuated total reflectance) FT-IR Spectroscopy

FT-IR spectra were recorded on an Agilent Technologies Cary 600 series instrument.

MALDI-TOF

Mass measurements of small molecules were recorded using a Shimadzu Biotech Axima Confidence MALDI-TOF mass spectrometer.

Single Crystal X-Ray Diffraction (SXRD)

SXRD data was collected for ANDI derivatives using a Bruker Kappa D8 Quest diffractometer. The Bruker Kappa D8 Quest diffractometer is equipped with an Incoatec microfocus Mo Kα radiation source, HELIOS multilayer optics, Oxford Cryosystems cryostream, and a Photon 100 CMOS detector. Bruker SAINT was used for all datasets for integration and scaling, SADABS was used for absorption correction (multi-scan) and analysis of systematic absences of hkl reflections and XPREP was used for space group selection. All initial models of compounds were

generated with SHELXT (intrinsic phasing method)[1] and least-squares refinement was carried out with SHELXL2014.2.[1, 2]

Powder X-Ray Diffraction (PXRD)

PXRD data was collected using a Rigaku Ultima III XRD equipped with Cu Kα radiation.

Temperature-dependent Powder X-Ray Diffraction (PXRD)

Temperature-dependent PXRD was collected using a Rigaku Ultima III XRD equipped with an HT 1500 high temperature attachment with Cu Kα radiation. Samples were placed on the sample holder, and measured with 2θ range from 2–40°. The temperature of the experiment was programmed from room temperature to 200 °C with a 10 °C/min heating rate. PXRD data was collected while the sample was heating to 200 °C.

Thermal Analysis

Thermal properties of BNDI samples were analyzed with differential scanning calorimetry (DSC) using a TA Instruments Q2000. The samples were heated from 0 °C to 240 °C at a heating rate of 10 K/min, under a flow of nitrogen (50 mL/min).

Hot-Stage Polarized Optical Microscopy

Thermo-mechanical behavior was analyzed using a MEIJI TECHNO ML9000 series polarizing microscope equipped with an Instech hot stage. The maximum temperature that the sample can be heated on this stage is 200 °C. The sample was placed on a 1 mm thick glass slide and the sample was cooled 0 °C by sending cooled nitrogen gas through the stage. The sample was then heated to 200 °C. The actual temperature of the stage was determined by a Phidget Temperature Sensor (P/N 1051_2).

3D Printed BNDI/PLA Filament

BNDI-T was mixed at 150°C with polylactic acid (PLA) at 1:19 and 1:9 w/w% until homogenous. Approximately 10 grams of BNDI-T:PLA at 1:19 were cut into small pieces to be inserted into a Filabot original benchtop extruder (Filabot, Barre, VT). The extruder was run at 170°C with pure PLA for 10 min. At the same temperature, the BNDI-T@PLA blend was added and extruded to obtain an average filament diameter of 2.35 mm. Dog bones were designed using the open source Blender software package (https://www.blender.org) and printed with a LulzBot TAZ 5 3D printer (Figure 6, Aleph Object, Inc., Loveland, CO). The printer was operated using the open source Cura software package for LulzBot. The printing parameters used to fabricate the thermochromic 3D printed objects are as such: print speed: 50 mm/s, layer height: 0.25 mm, shell thickness: 0.50 mm, retraction speed: 10 mm/s, travel speed: 175 mm/s, bottom layer speed: 15 mm/s, infill speed: 30 mm/s, top/bottom speed: 35 mm/s, outer shell speed: 35 mm/s, and inner shell speed: 35 mm/s. The temperature of the hot end was set at 190°C, and the temperature of the print bed was set to 65 °C. A print head with a 0.50 mm nozzle diameter was used. Filaments were also extruded with BNDI-T@PLA at 1:19 w/w% and with HxNDI@PLA at 1:9 w/w %. to print thermochromic dog bones (Figure 7).

Synthesis and Characterization

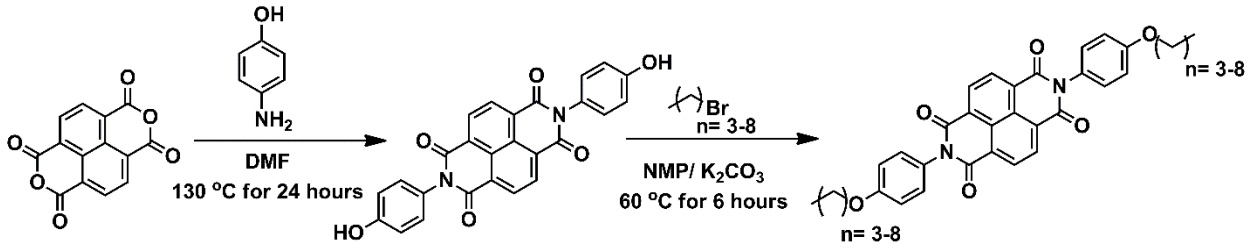

Scheme S1. Synthesis of alkoxyphenyl N-substituted naphthalene diimides discussed in this study.

Synthesis of NDI-Ph

Phenyl N-substituted naphthalene diimide (NDI-Ph) was prepared as shown in **Scheme S1**. A mixture of 1,4,5,8-naphthalenetetracarboxylic dianhydride (4.582 g, 2.119 mmol and 4-aminophenol (4.627 g, 4.240 mmol) was heated under reflux at 130 °C for 24 h. The reaction product was then collected under filtration and washed with dimethylformamide. ^{1}H-NMR (600 MHz, DMSO-D_6, ppm) (Figure S1): 6.90 (d, 8.6 Hz, 4H), 7.22 (d, 8.3 Hz, 4 H), 8.85 (s, 4 H). ^{13}C-NMR (600 MHZ, DMSO-D_6, ppm) (Figure S2): 39.38, 39.52, 39.66, 115.46, 126.39, 126.96, 129.84, 130.41, 157.36, 163.11. MALDI-MS: calculated for $C_{36}H_{34}N_2O_6$ is 450.09 obtained m/z = 450.05 (M^+).

Synthesis of BNDI

Butoxyphenyl N-substituted naphthalene diimide (BNDI) was prepared using a previously described method.[3]

Synthesis of PNDI

Pentoxyphenyl N-substituted naphthalene diimide (PNDI) was prepared as shown in **Scheme S1**. NDI-Phenol (1.980 g, 4.400 mmol) was mixed with 1-bromopentane (1.330 g, 8.800 mmol) in 1-methyl-2-pyrrolidinone (80.00 mL) and heated to 70 °C for 6 h. The reaction mixture was poured into diluted hydrochloric acid and a precipitate was observed, filtered under vacuum, and purified using column chromatography (hexane-DCM) with a 60.11% yield. ^{1}H-NMR (600 MHz, $CDCl_3$, ppm) (**Figure S3**): 0.94 (t, 7.3 Hz, 6 H), 1.40 (s, 7.3 Hz, 4 H), 1.46 (q, 7.8 Hz, 4 H), 1.82 (q, 7.1 Hz, 4 H), 4.01 (t, 6.5 Hz, 4 H), 7.06 (d, 8.4 Hz, 4 H), 7.22 (d, 8.4 Hz, 4 H), 8.81 (s, 4H). ^{13}C-NMR (600 MHZ, $CDCl_3$, ppm) (**Figure S4**): 14.19, 22.61, 28.37, 29.09, 68.42, 76.95, 77.16, 77.37, 115.53, 126.81, 127.20, 127.32, 129.47, 131.56, 159.70, 163.36. MALDI-MS: calculated for $C_{36}H_{34}N_2O_6$ is 590.24 obtained m/z = 590.49 (M^+).

Synthesis of HxNDI

Hexoxyphenyl N-substituted naphthalene diimide (HxNDI) was prepared according to our previously published literature with a 63.02% yield. ^{1}H-NMR (600 MHz, $CDCl_3$, ppm) (**Figure S5**): 0.93 (t, 6.3 Hz, 6 H), 1.37 (m, 3.7 Hz, 8 H), 1.50 (q, 7.9 Hz, 4 H), 1.83 (q, 7.5 Hz, 4 H), 4.03 (t, 7.6 Hz, 4 H), 7.08 (d, 8.6 Hz, 4 H), 7.24 (d, 8.5 Hz, 4 H), 8.83 (s, 4H). ^{13}C-NMR (600 MHZ, $CDCl_3$, ppm) (**Figure S6**): 14.20, 22.77, 25.89, 29.35, 31.72, 68.43, 76.95, 77.16, 77.37, 115.52, 126.80, 127.19, 127.31, 129.47, 131.55, 159.70, 163.35. MALDI-MS: calculated for $C_{38}H_{38}N_2O_6$ is 618.27 obtained m/z = 618.48 (M^+).

Synthesis of HNDI

Heptoxyphenyl N-substituted naphthalene diimide (HNDI) was prepared as shown in **Scheme S1**. NDI-Phenol (1.980 g, 4.400 mmol) was mixed with 1-bromoheptane (1.576 g, 8.800 mmol) in 1-methyl-2-pyrrolidinone (80.00 mL) and heated to 70 °C for 6 hours. The reaction mixture was poured into diluted hydrochloric acid and a precipitate was observed, filtered under vacuum, and purified using column chromatography (hexane-DCM) with a 63.02% yield. ^{1}H-NMR (600 MHz, $CDCl_3$, ppm) (**Figure S7**): 0.89 (t, 6.9 Hz, 6 H), 1.32 (m, 7.7 Hz, 8 H), 1.37 (m, 7.7 Hz, 4 H), 1.47 (q, 7.6 Hz, 4 H), 1.81 (q, 7.4 Hz, 4 H), 4.01 (t, 6.6 Hz, 4 H), 7.06 (d, 8.4 Hz, 4 H), 7.22 (d, 8.3 Hz, 4 H), 8.81 (s, 4H). ^{13}C-NMR (600 MHZ, $CDCl_3$, ppm) (**Figure S8**): 14.26, 22.78, 26.18, 29.21, 29.39, 31.95, 68.44, 76.95, 77.16, 77.37, 115.53, 126.80, 127.20, 127.31, 129.47, 131.56, 159.71, 163.35. MALDI-MS: calculated for $C_{40}H_{42}N_2O_6$ is 646.30 obtained m/z = 646.54 (M^+).

Synthesis of ONDI

Octoxyphenyl N-substituted naphthalene diimide (ONDI) was prepared as shown in **Scheme S1**. NDI-Phenol (1.980 g, 4.400 mmol) was mixed with 1-bromooctane (1.699 g, 8.800 mmol) in 1-methyl-2-pyrrolidinone (80.00 mL) and heated to 70 °C for 6 hours. The reaction mixture was

poured into diluted hydrochloric acid and a precipitate was observed, filtered under vacuum, and purified using column chromatography (hexane-DCM) with a 62.75% yield. 1H-NMR (600 MHz, CDCl3, ppm) (Figure S9): 0.91 (t, 6.9 Hz, 6H), 1.33 (m, 6.5 Hz, 16 H), 1.49 (q, 7.7 HZ, 4 H), 1.83 (q, 7.6 Hz, 4 H), 4.03 (t, 6.6 Hz, 4 H), 7.08 (d, 8.8 HZ, 4 H), 7.24 (d, 8.6 Hz, 4 H), 8.84 (s, 4 H). ^{13}C-NMR (600 MHZ, $CDCl_3$, ppm) (**Figure S10**): 14.27, 22.83, 26.23, 29.40, 29.41, 29.51, 31.99, 68.45, 76.95, 77.16, 77.37, 115.54, 126.81, 127.21, 127.33, 129.48, 131.56, 159.72, 163.35. MALDI-MS: calculated for $C_{42}H_{46}N_2O_6$ is 674.34 obtained m/z = 674.15 (M^+).

Synthesis of NNDI

Nonoxyphenyl N-substituted naphthalene diimide (NNDI) was prepared as shown in **Scheme S1**. NDI-Phenol (1.980 g, 4.400 mmol) was mixed with 1-bromononane (1.820 g, 8.800 mmol) in 1-methyl-2-pyrrolidinone (80.00 mL) and heated to 70 °C for 6 hours. The reaction mixture was poured into diluted hydrochloric acid and a precipitate was observed, filtered under vacuum, and purified using column chromatography (hexane-DCM) with a 69.57% yield. ^{1}H-NMR (600 MHz, $CDCl_3$, ppm) (**Figure S11**): 0.90 (t, 7.0 Hz, 6 H), 1.33 (m, 6.1 Hz, 20 H), 1.49 (q, 7.3 Hz, 4 H), 1.83 (q, 7.3 Hz, 4 H), 4.03 (t, 6.2 Hz, 4 H), 7.08 (d, 8.4 Hz, 4 H), 7.24 (d, 8.4 Hz, 4 H), 8.83 (s, 4 H). ^{13}C-NMR (600 MHZ, $CDCl_3$, ppm) (**Figure S12**): 14.27, 22.84, 26.22, 29.39, 29.44, 29.55, 29.71, 32.04, 76.95, 77.16, 77.37, 115.53, 126.81, 127.20, 127.32, 129.47, 131.56, 159.71, 163.35. MALDI-MS: calculated for $C_{44}H_{50}N_2O_6$ is 702.37 obtained m/z = 702.56 (M^+).

Crystal data for HxNDI. $C_{38}H_{38}N_2O_6$, M_r = 618.7, monoclinic, a = 8.395(3), b = 8.853(3), c = 23.938(9) Å, α = 89.528(11), β = 80.712(14), γ = 62.60(2)°, V = 1554.3(10) Å^3, T = 100 K, space group $P\overline{1}$, Z = 2, μ = 0.09 mm^{-1}, 20000 reflections measured, 7191 unique (R_{int} = 0.044) which were used in all calculations. The final wR(2) was 0.133 (all data) and R(1) was 0.055 (>2σ(I)). CCDC deposition number 1839983.

Crystal data for HNDI at 100 K. $C_{40}H_{42}N_2O_6$, M_r = 646.75, monoclinic, *a* = 4.1696(15), *b* = 46.595(14), *c* = 8.214(3) Å, *α* = 90, *β* = 93.529(10), *γ* = 90°, *V* = 1592.7(9) Å^3, T = 100 K, space group $P2_1$, Z = 2, μ = 0.09 mm^{-1}, 40965 reflections measured, 3672 unique (R_{int} = 0.060) which were used in all calculations. The final wR(2) was 0.104 (all data) and R(1) was 0.046 (>2σ(I)). CCDC deposition number 1839985.

Crystal data for HNDI at 200 K. $C_{40}H_{42}N_2O_6$, M_r = 646.75, monoclinic, *a* = 4.2455(15), *b* = 46.493(15), *c* = 8.218(2) Å, *α* = 90, *β* = 93.584(8), *γ* = 90°, *V* = 1619.0(9) Å^3, T = 200 K, space group $P2_1$, Z = 2, μ = 0.09 mm^{-1}, 40092 reflections measured, 3732 unique (R_{int} = 0.054) which were used in all calculations. The final wR(2) was 0.109 (all data) and R(1) was 0.047 (>2σ(I)). CCDC deposition number 1857158.

Crystal data for HNDI at 298 K. $C_{40}H_{42}N_2O_6$, M_r = 646.75, monoclinic, *a* = 4.3773(18), *b* = 46.183(15), *c* = 8.215(3) Å, *α* = 90, *β* = 93.759(6), *γ* = 90°, *V* = 1657.2(10) Å^3, T = 298 K, space group $P2_1$, Z = 2, μ = 0.09 mm^{-1}, 40572 reflections measured, 3820 unique (R_{int} = 0.066) which were used in all calculations. The final wR(2) was 0.127 (all data) and R(1) was 0.051 (>2σ(I)). CCDC deposition number 1857159.

Crystal data for ONDI at 100 K. $C_{42}H_{46}N_2O_6$, M_r = 674.81, triclinic, *a* = 4.1680(14), *b* = 8.217(3), *c* = 24.901(7) Å, *α* = 97.81(1), *β* = 93.453(7), *γ* = 93.834(6)°, *V* = 841.0(5) Å^3, T = 100 K, space group $P\bar{1}$, Z = 1, μ = 0.09 mm^{-1}, 25306 reflections measured, 3887 unique (R_{int} = 0.076) which were used in all calculations. The final wR(2) was 0.120 (all data) and R(1) was 0.054 (>2σ(I)). CCDC deposition number 1839986.

Crystal data for ONDI at 200 K. $C_{42}H_{46}N_2O_6$, M_r = 674.81, triclinic, *a* = 4.2498(17), *b* = 8.217(3), *c* = 24.826(7) Å, *α* = 97.903(9), *β* = 93.317(9), *γ* = 93.732(8)°, *V* = 854.9(5) Å^3, T = 200 K, space group $P\bar{1}$, Z = 1, μ = 0.09 mm^{-1}, 21943 reflections measured, 3953 unique (R_{int} = 0.068) which

were used in all calculations. The final wR(2) was 0.130 (all data) and R(1) was 0.057 (>2σ(I)). CCDC deposition number 1857160.

Crystal data for ONDI at 298 K. $C_{42}H_{46}N_2O_6$, M_r = 674.81, triclinic, *a* = 4.3797(17), *b* = 8.220(3), *c* = 24.683(8) Å, *α* = 98.313(13), *β* = 93.051(8), *γ* = 93.777(6)°, *V* = 875.6(6) Å^3, T = 298 K, space group $P\bar{1}$, Z = 1, μ = 0.09 mm^{-1}, 28393 reflections measured, 4061 unique (R_{int} = 0.089) which were used in all calculations. The final wR(2) was 0.143 (all data) and R(1) was 0.061 (>2σ(I)). CCDC deposition number 1857161.

Crystal data for NNDI at 100 K. $C_{44}H_{50}N_2O_6$, M_r = 702.86, monoclinic, *a* = 4.154(2), *b* = 51.72(2), *c* = 8.253(3) Å, *α* = 90(1), *β* = 93.663(12), *γ* = 90°, *V* = 1769.6(14) Å^3, T = 100 K, space group $P2_1$, Z = 2, μ = 0.09 mm^{-1}, 36862 reflections measured, 4080 unique (R_{int} = 0.095) which were used in all calculations. The final wR(2) was 0.118 (all data) and R(1) was 0.055 (>2σ(I)). CCDC deposition number 1839987.

Crystal data for NNDI at 200 K. $C_{44}H_{50}N_2O_6$, M_r = 702.86, monoclinic, *a* = 4.2348(19), *b* = 51.591(19), *c* = 8.261(3) Å, *α* = 90(1), *β* = 93.622(11), *γ* = 90°, *V* = 1801.1(13) Å^3, T = 200 K, space group $P2_1$, Z = 2, μ = 0.09 mm^{-1}, 25071 reflections measured, 4162 unique (R_{int} = 0.114) which were used in all calculations. The final wR(2) was 0.163 (all data) and R(1) was 0.084 (>2σ(I)). CCDC deposition number 1857162.

Crystal data for NNDI at 298 K. $C_{44}H_{50}N_2O_6$, M_r = 702.86, monoclinic, *a* = 4.362(3), *b* = 51.35(4), *c* = 8.268(5) Å, *α* = 90(1), *β* = 93.56(2), *γ* = 90°, *V* = 1848(2) Å^3, T = 200 K, space group $P2_1$, Z = 2, μ = 0.08 mm^{-1}, 30722 reflections measured, 4263 unique (R_{int} = 0.103) which were used in all calculations. The final wR(2) was 0.148 (all data) and R(1) was 0.066 (>2σ(I)). CCDC deposition number 1857163.

Table S1. VTSXRD data for HNDI

Temperature/ K	100	200	298
Crystal system	monoclinic	monoclinic	monoclinic
Space group	$P2_1/n$	$P2_1/n$	$P2_1/n$
a =	4.1696(15)	4.2455(15)	4.3773(18)
b =	46.595(14)	46.493(15)	46.183(15)
Unit cell/Å ***c*** =	8.214(3)	8.218(2)	8.215(3)
α =	90°	90°	90°
β =	93.529(10)°	93.584(7)°	93.759(6)°
γ =	90°	90°	90°
Volume/ Å^3	1592.7(9)	1619.0.0(9)	1657.2(10)
Z	2	2	2
Reflections collected	40965	40092	40572
R_{int}	0.060	0.054	0.066
Calculated density/Mg m^{-3}	1.349	1.327	1.296
Extinction coefficient	0.0042(11)	0.0076 (13)	0.0114(17)
***R*[$F^2 > 2\sigma(F^2)$]**	0.046	0.047	0.051
***wR*(F^2)**	0.104	0.109	0.127

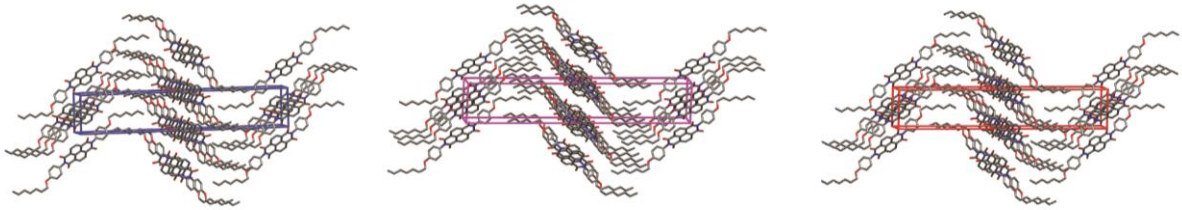

Table S2. VTSXRD data for ONDI

Temperature/ K		100	200	298
Crystal system		triclinic	triclinic	triclinic
Space group		$P\bar{1}$	$P\bar{1}$	$P\bar{1}$
Unit cell/Å	***a*** =	4.1680(14)	4.2498(17)	4.3797(17)
	b =	8.217(3)	8.217(3)	8.220(3)
	c =	24.901(7)	24.826(7)	24.683(7)
	α =	97.81(1)°	97.903(9)°	98.313(9)°
	β =	93.453(7)°	93.317(9)°	93.051(9)°
	γ =	93.834(6)°	93.732(8)°	93.711(8)°
Volume/ Å^3		841.0(5)	854.9(5)	875.6(6)
Z		1	1	1
Reflections collected		20306	21943	28393
R_{int}		0.076	0.068	0.089
Calculated density/Mg m^{-3}		1.332	1.311	1.280
Extinction coefficient		0.012(2)	0.016(3)	0.017(3)
***R*[$F^2 > 2\sigma(F^2)$]**		0.054	0.057	0.061
***wR*(F^2)**		0.120	0.130	0.143

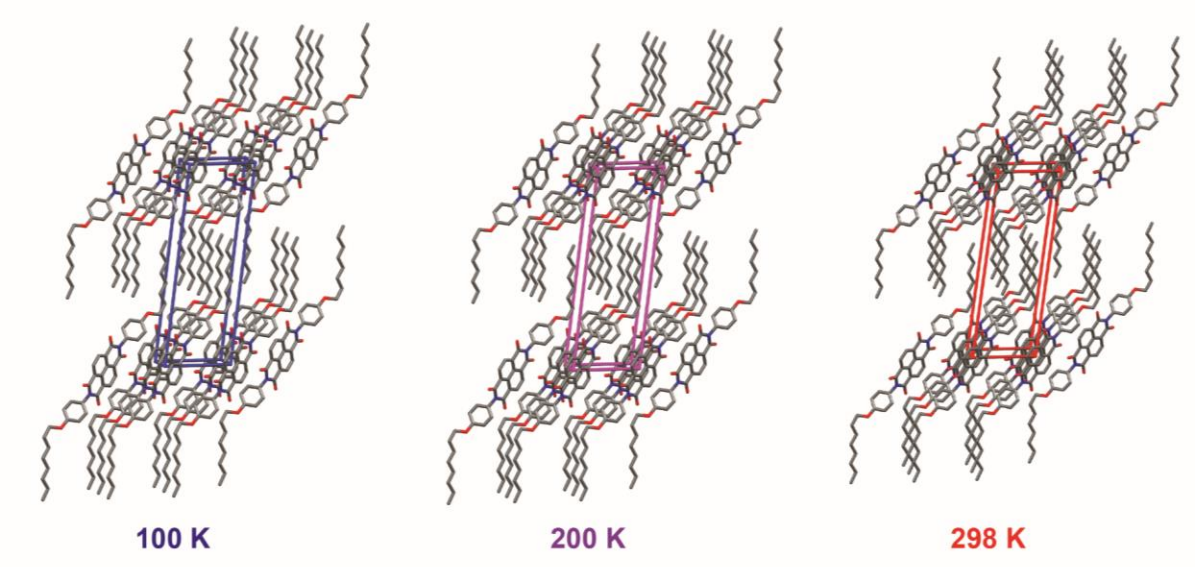

Table S3. VTSXRD data for NNDI

Temperature/ K		100	200	298
Crystal system		monoclinic	monoclinic	monoclinic
Space group		$P2_1/n$	$P2_1/n$	$P2_1/n$
Unit cell/Å	***a*** =	4.154(2)	4.235(19)	4.362(2)
	b =	51.72(2)	51.59(19)	51.35(4)
	c =	8.253(3)	8.261(3)	8.268(5)
	α =	90°	90°	90°
	β =	93.663(12)°	93.662(11)°	93.56(2)°
	γ =	90°	90°	90°
Volume/ Å^3		1769.6(14)	1801.1(13)	1848(2)
Z		2	2	2
Reflections collected		36862	25071	30722
R_{int}		0.095	0.114	0.103
Calculated density/Mg m^{-3}		1.319	1.296	1.263
$R[F^2 > 2\sigma(F^2)]$		0.055	0.084	0.066
$wR(F^2)$		0.118	0.163	0.148

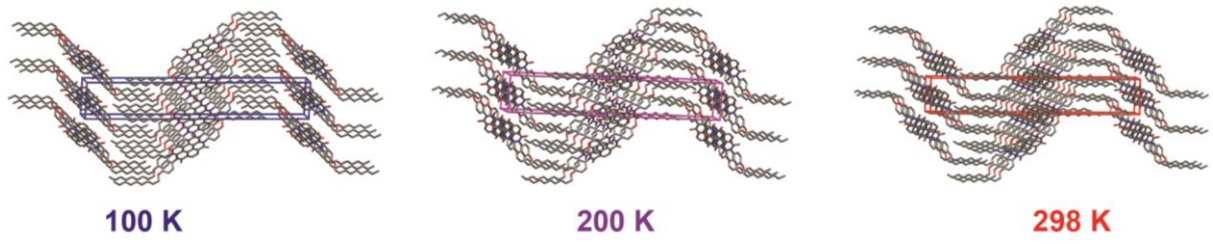

Figures

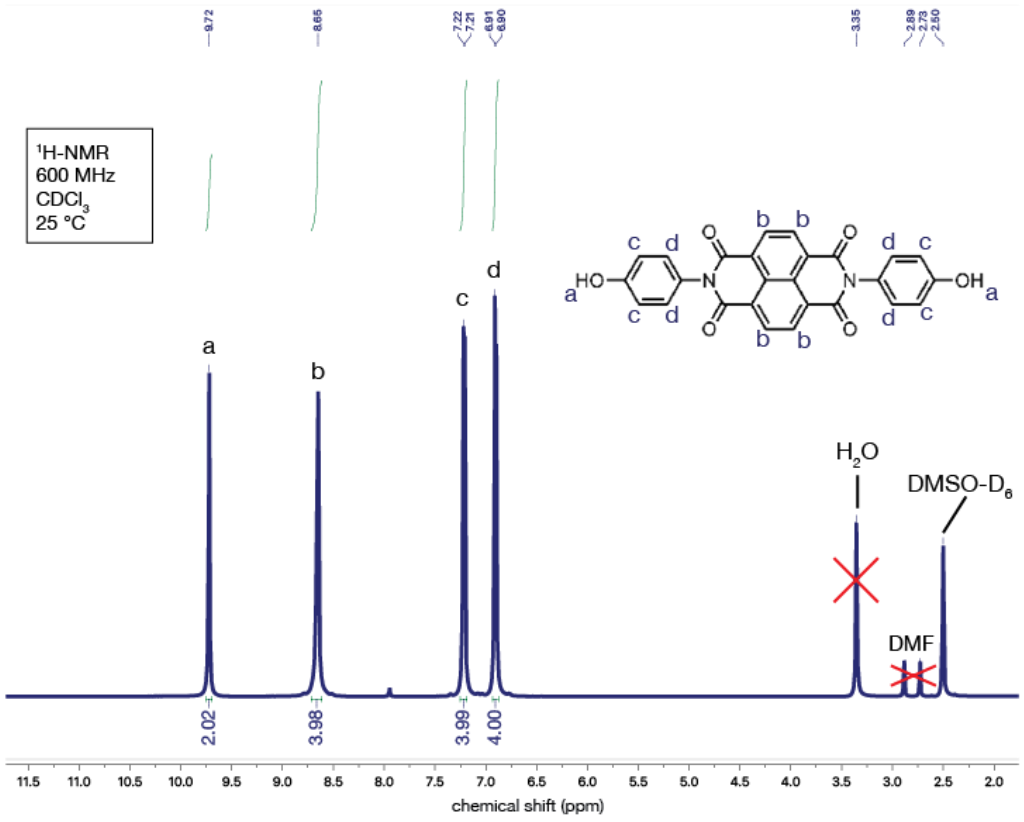

Figure S1: ^{1}H NMR spectrum of NDI-Ph.

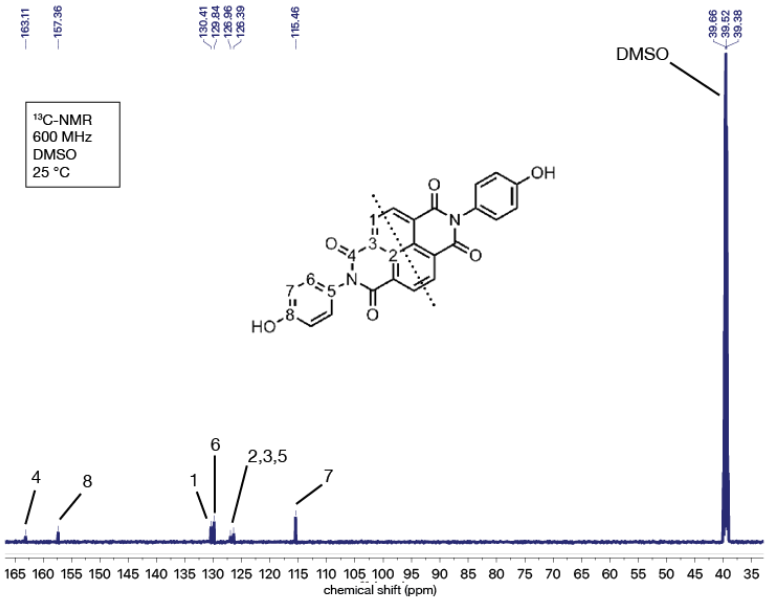

Figure S2: ^{13}C-NMR spectrum of NDI-Phenol.

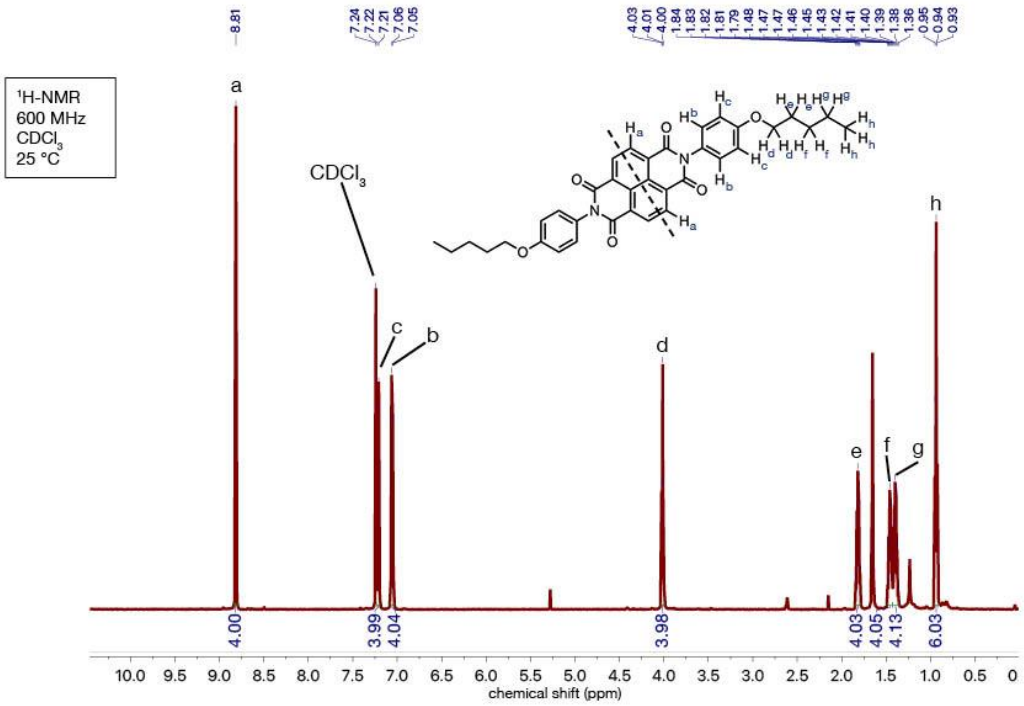

Figure S3: ^{1}H NMR spectrum of PNDI.

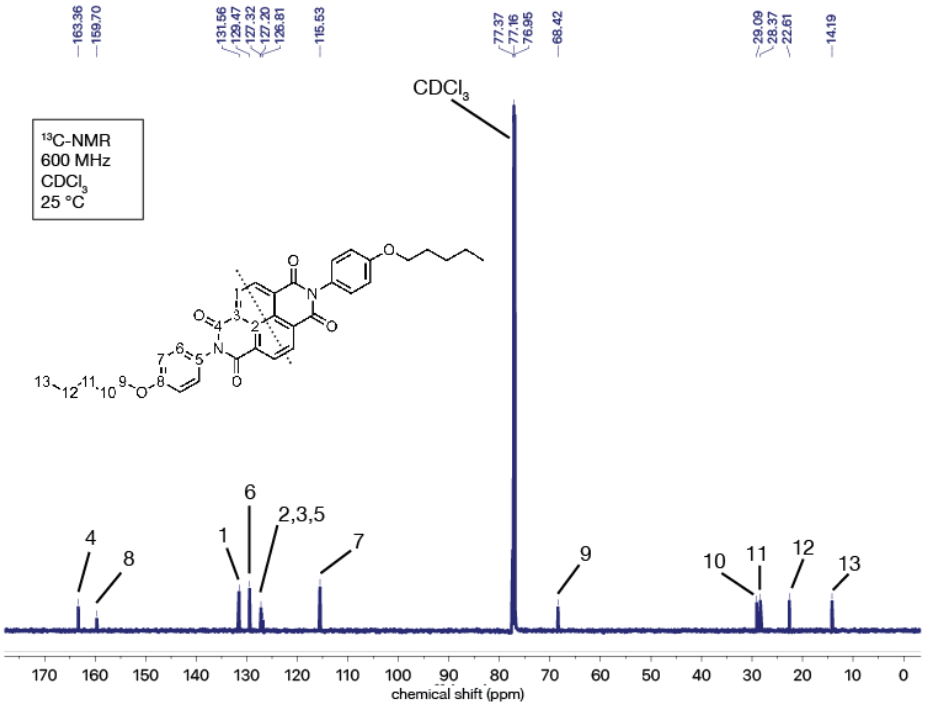

Figure S4: ^{13}C-NMR spectrum of PNDI.

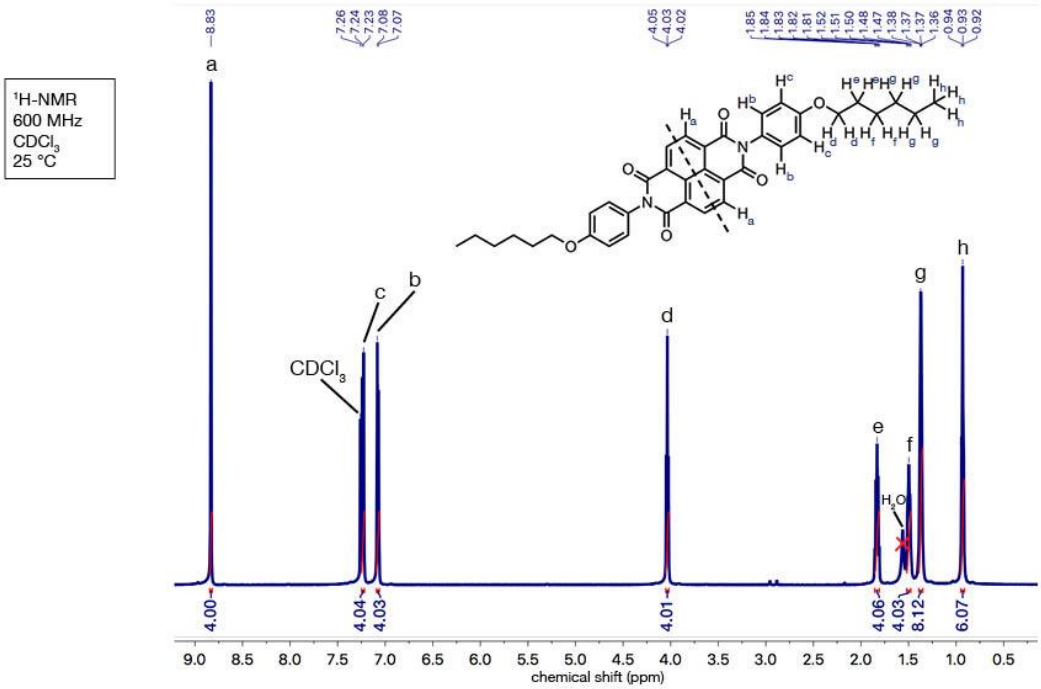

Figure S5: ^{1}H NMR spectrum of HxNDI.

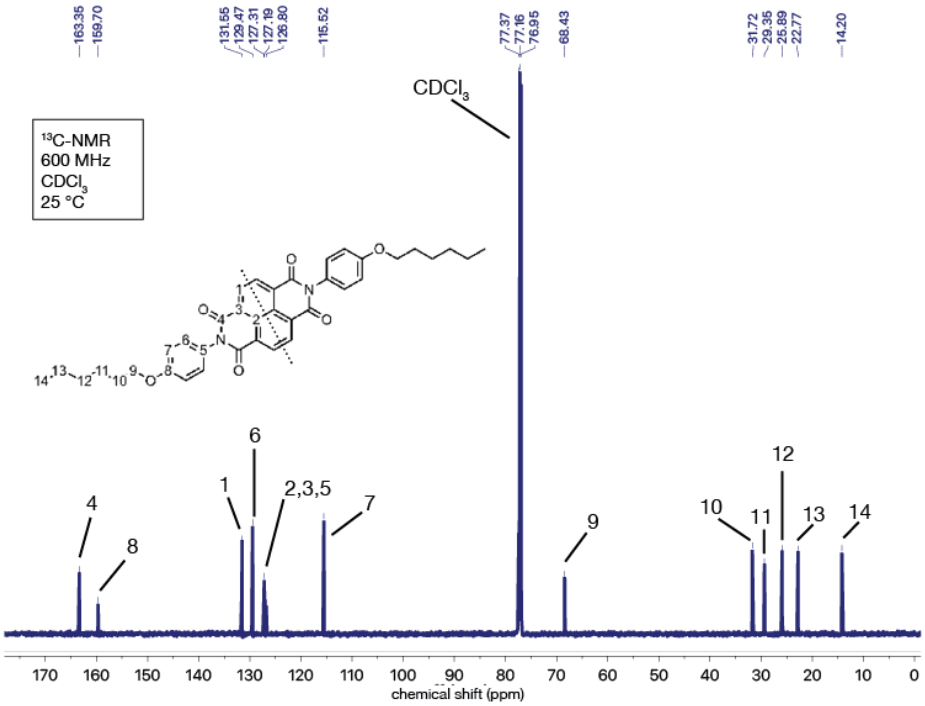

Figure S6: ^{13}C NMR spectrum of HxNDI.

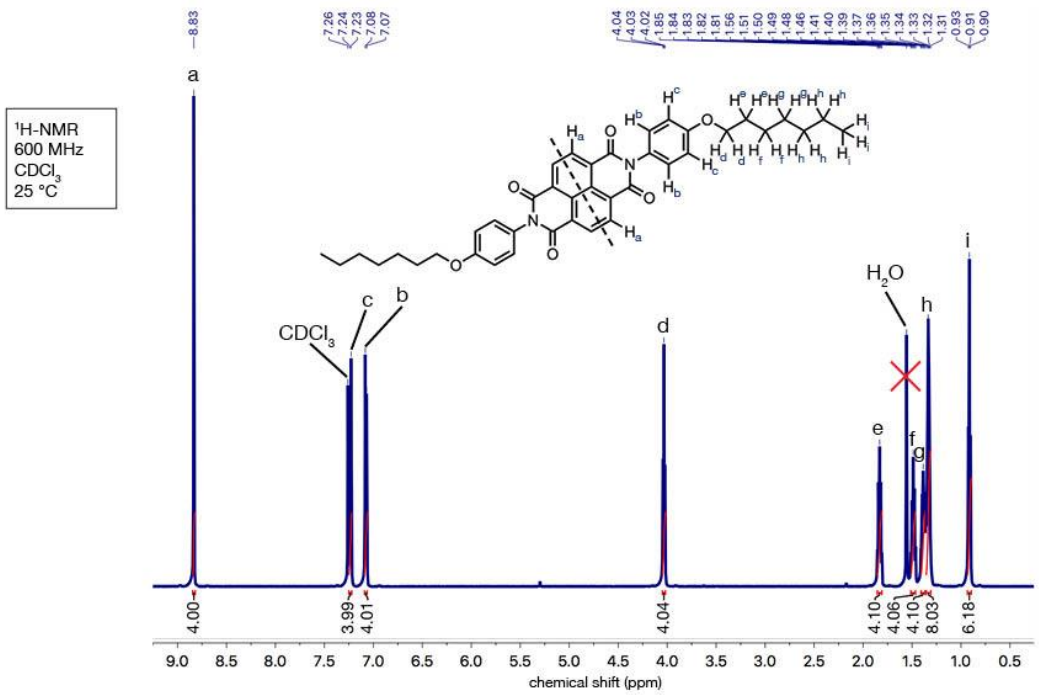

Figure S7: ^{1}H NMR spectrum of HNDI.

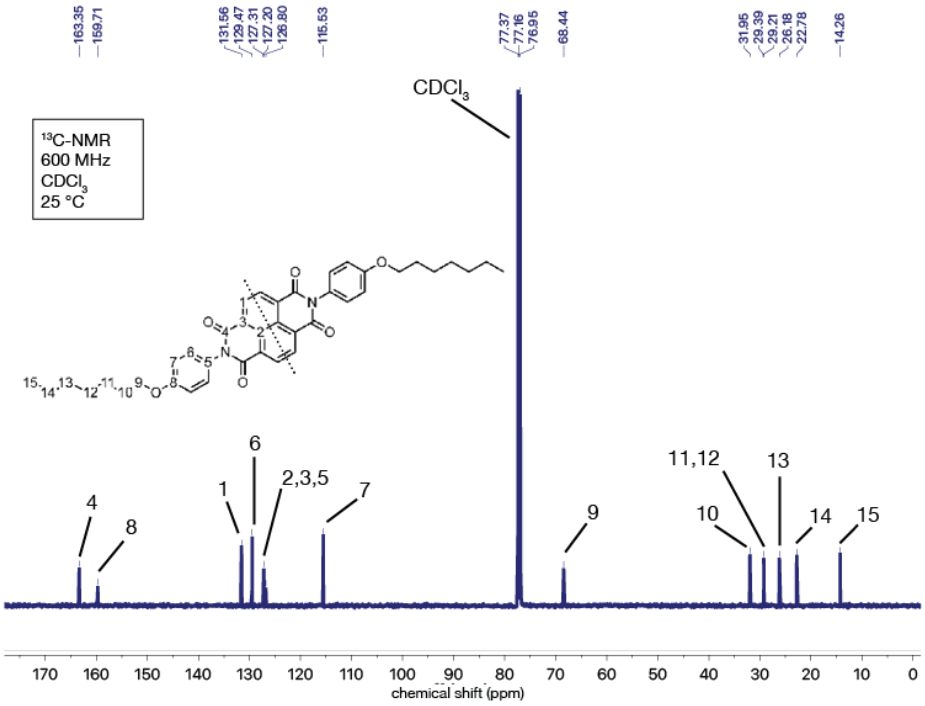

Figure S8: ^{13}C-NMR spectrum of HNDI.

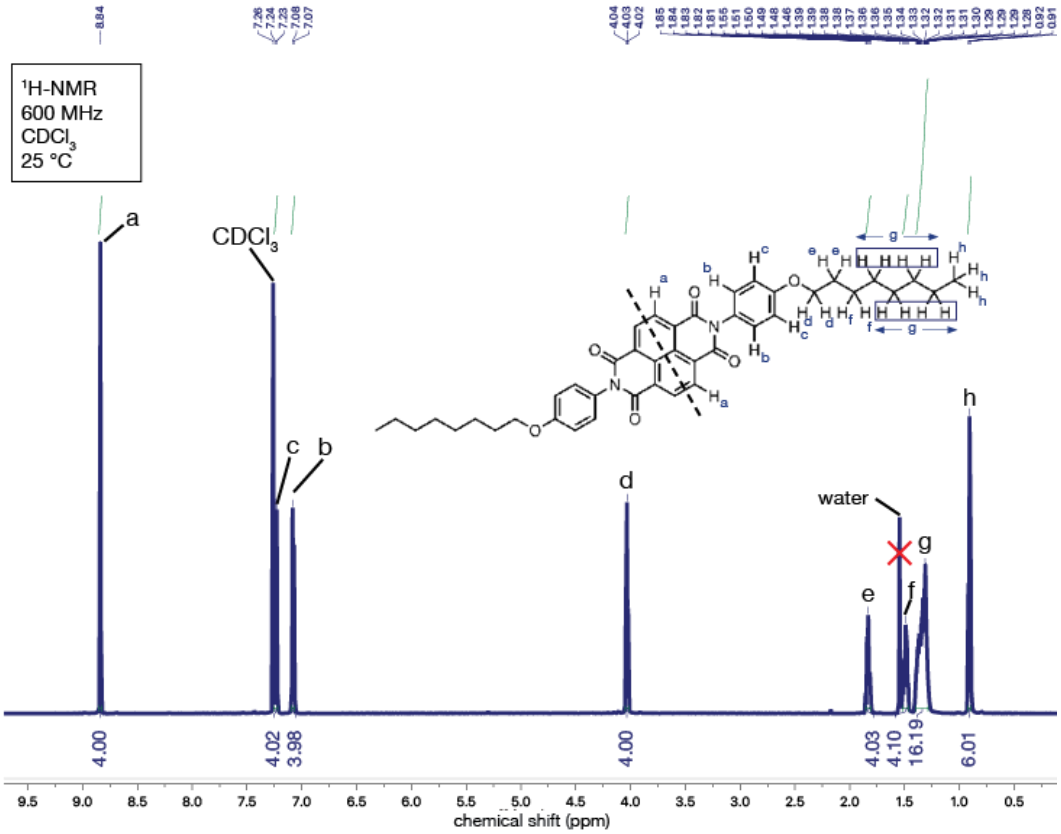

Figure S9: ^{1}H NMR spectrum of ONDI.

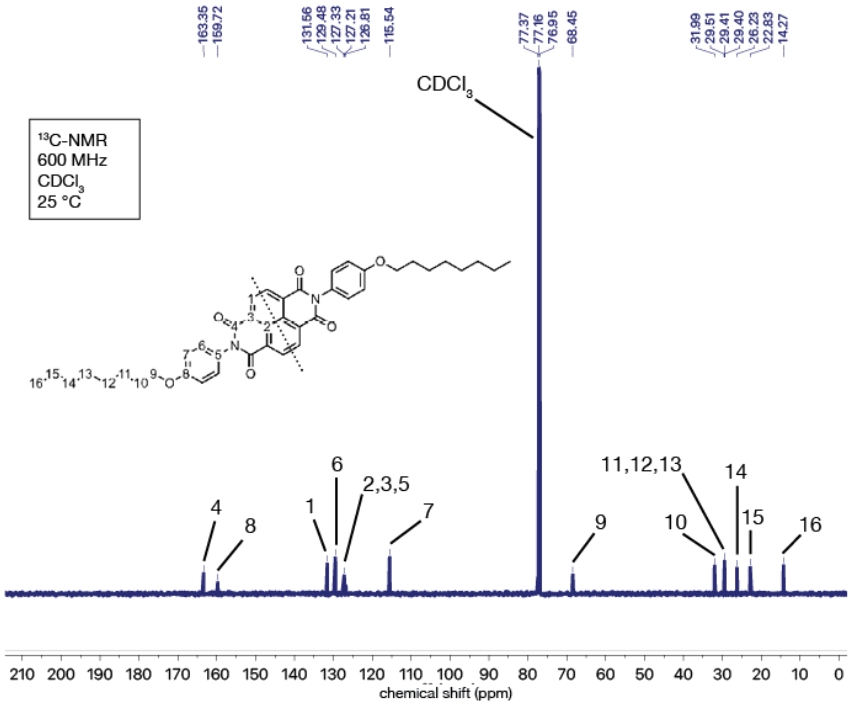

Figure S10: ^{13}C-NMR spectrum of ONDI.

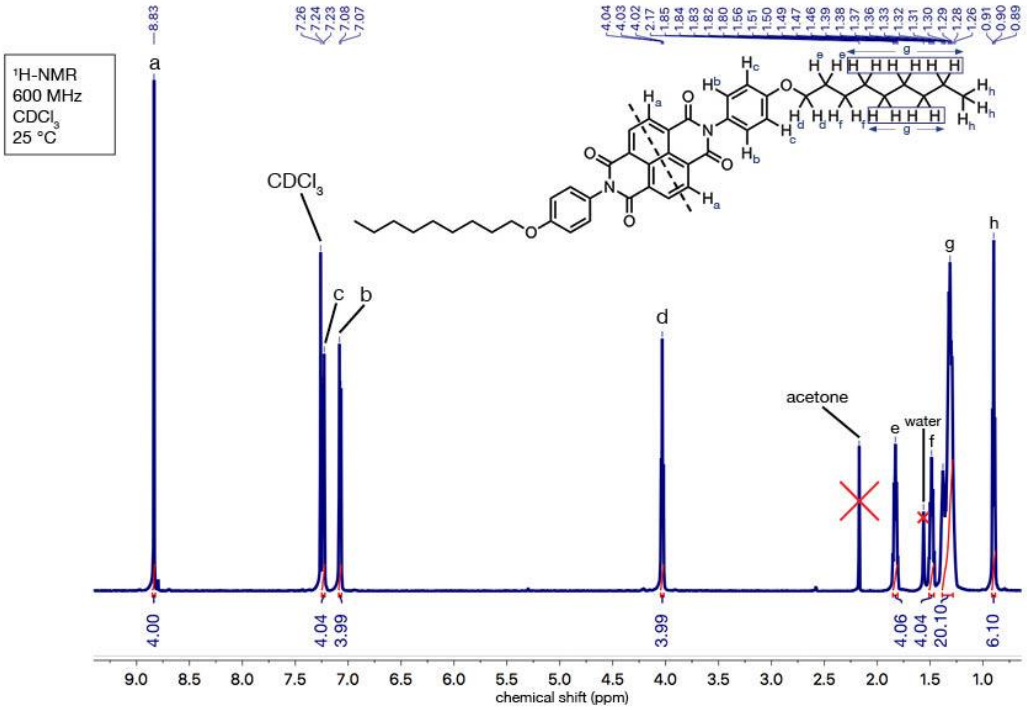

Figure S11: ^{1}H NMR spectrum of NNDI.

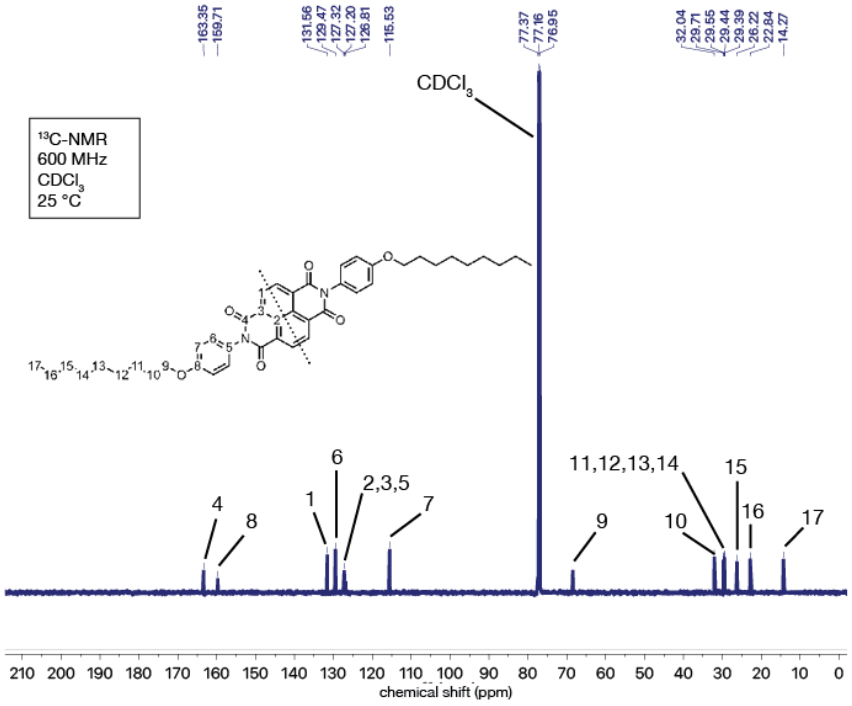

Figure S12: ^{13}C-NMR spectrum of NNDI.

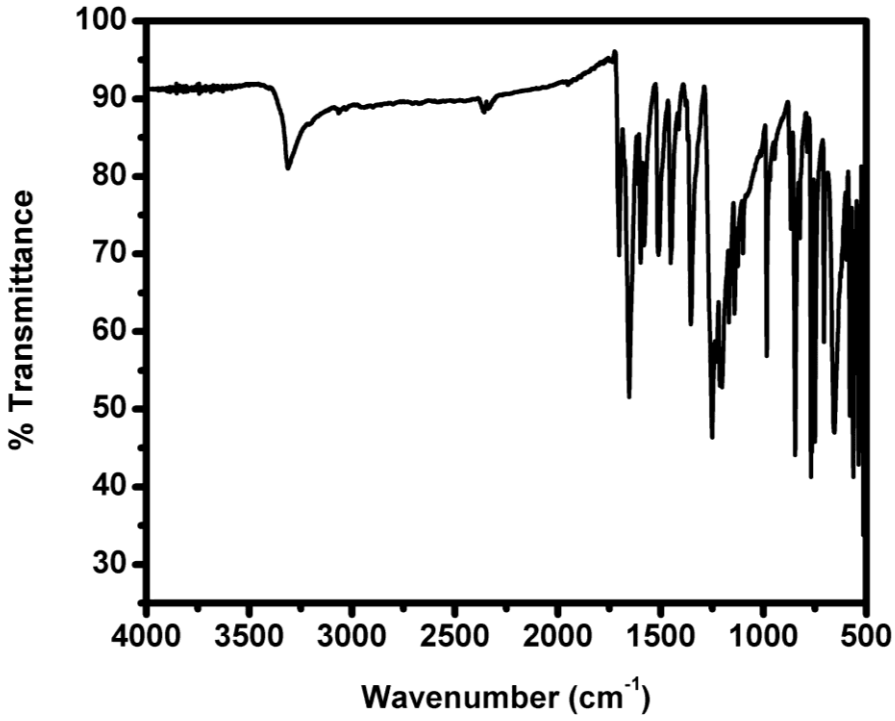

Figure S13. IR spectrum of NDI-Ph

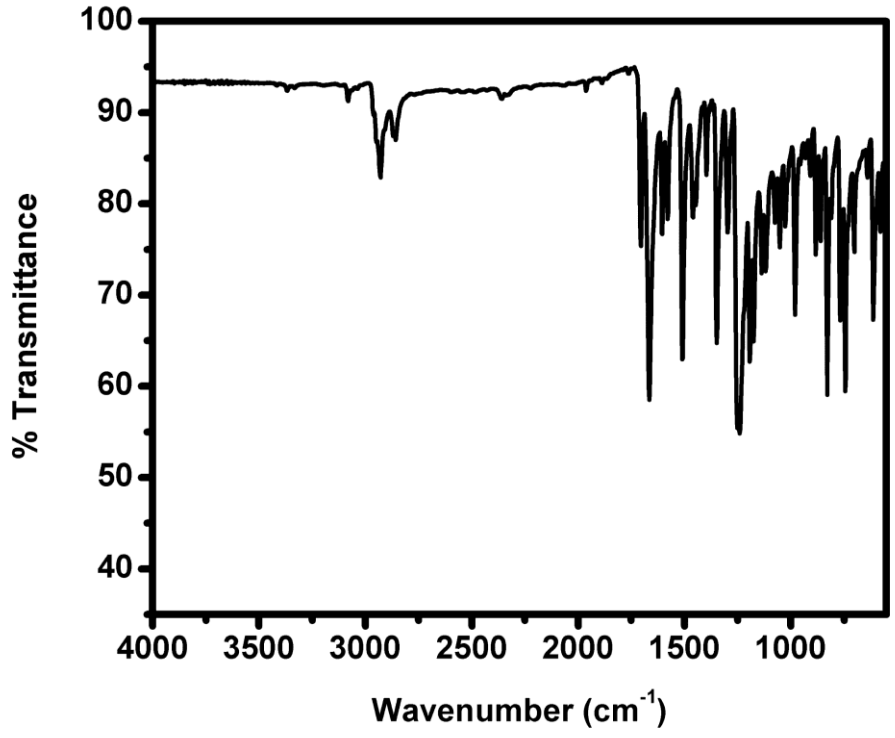

Figure S14. IR spectrum of PNDI

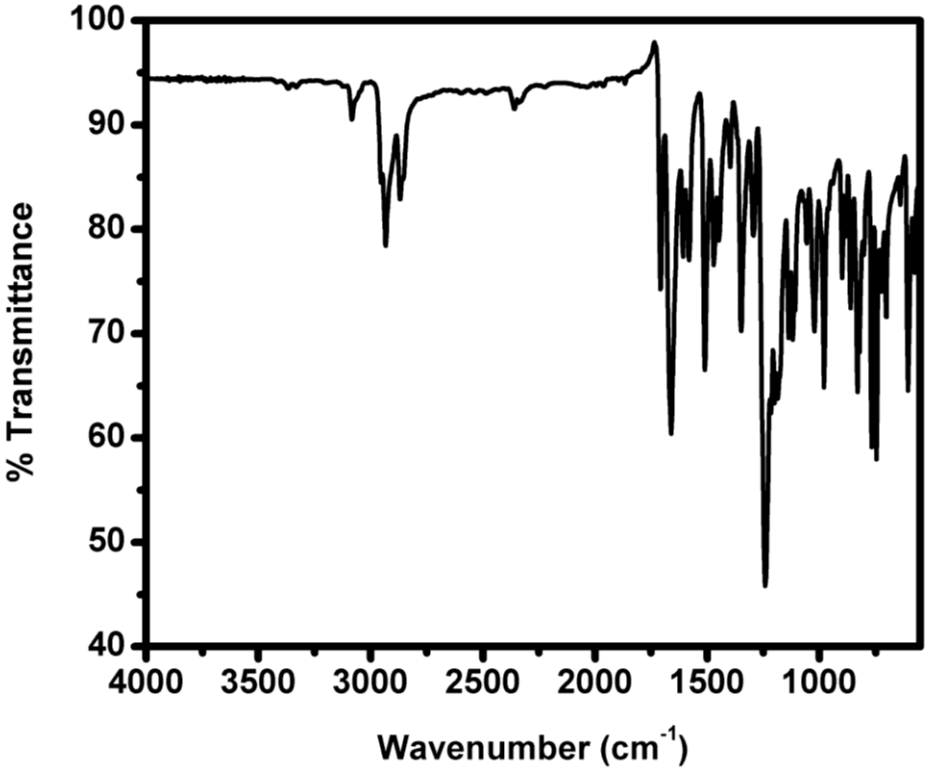

Figure S15. IR spectrum of HxNDI

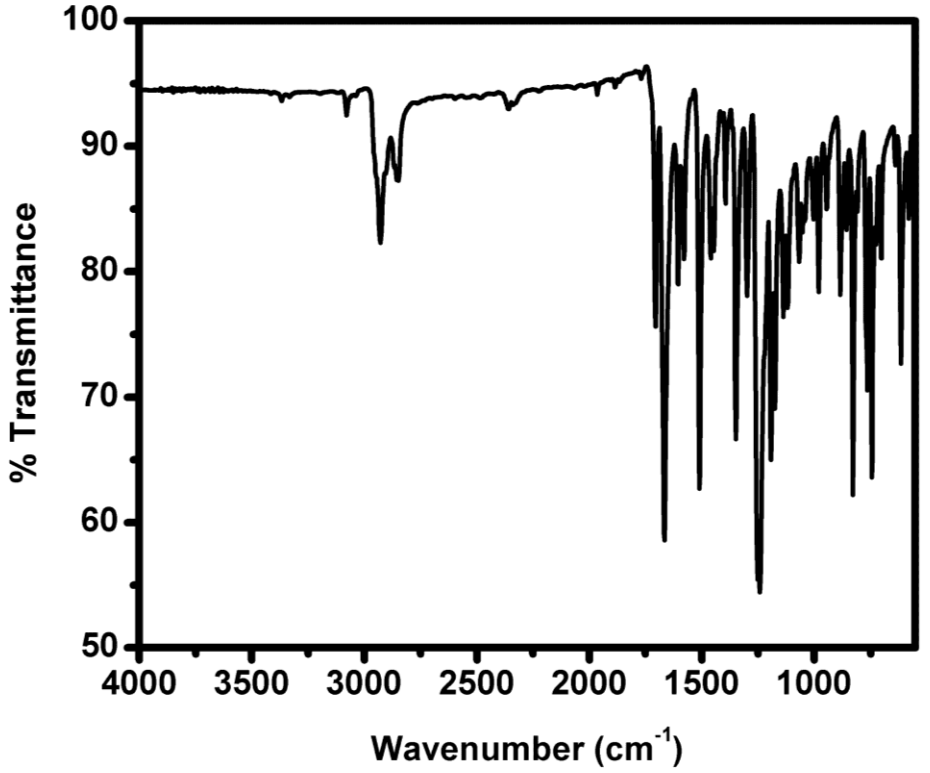

Figure S16. IR spectrum of HNDI

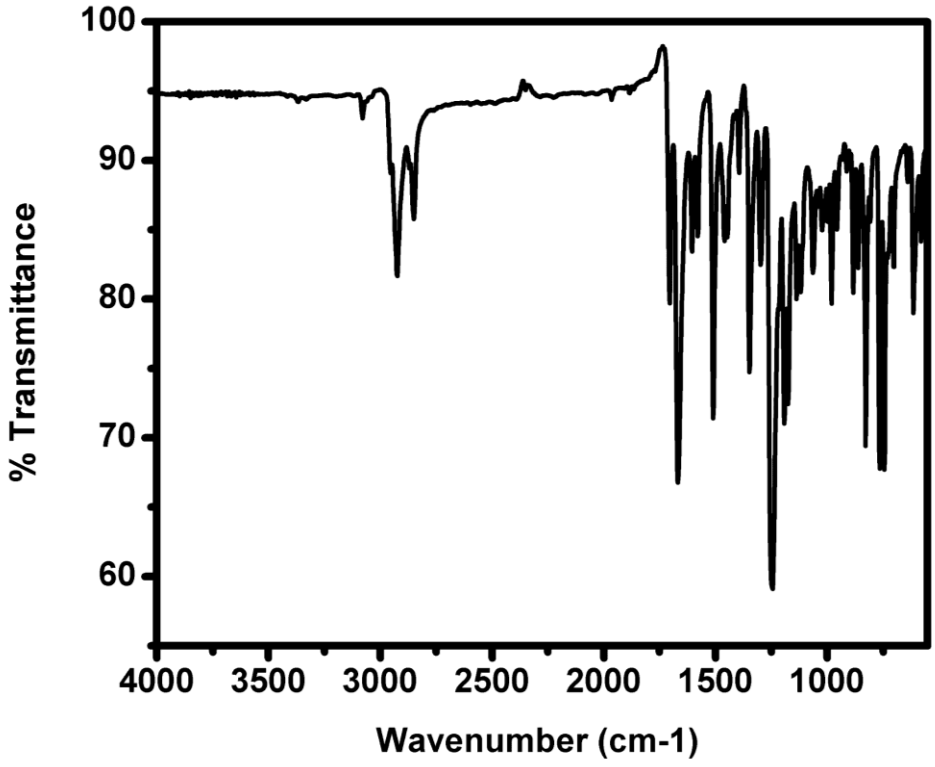

Figure S17. IR spectrum of ONDI

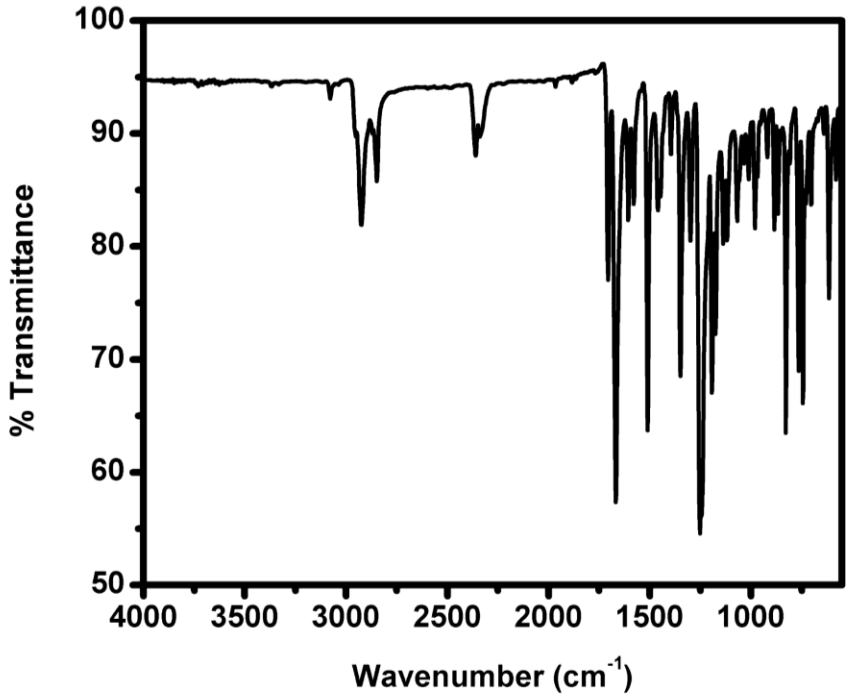

Figure S18. IR spectrum of NNDI. The signal observed near 2300 cm^{-1} is due to carbon dioxide in the atmosphere.

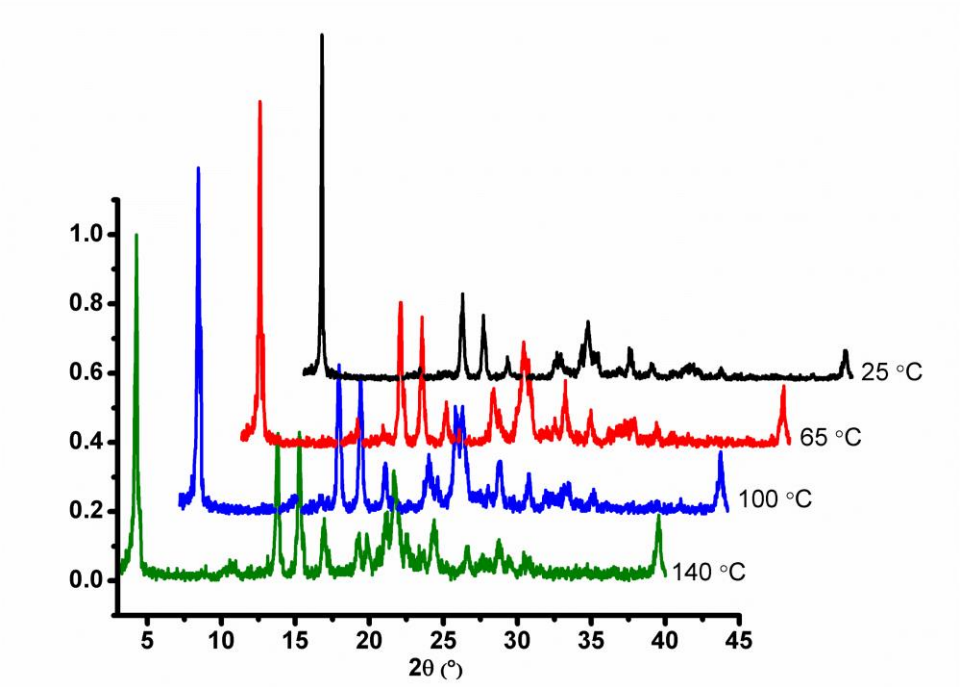

Figure S19. VTPXRD analysis of PNDI

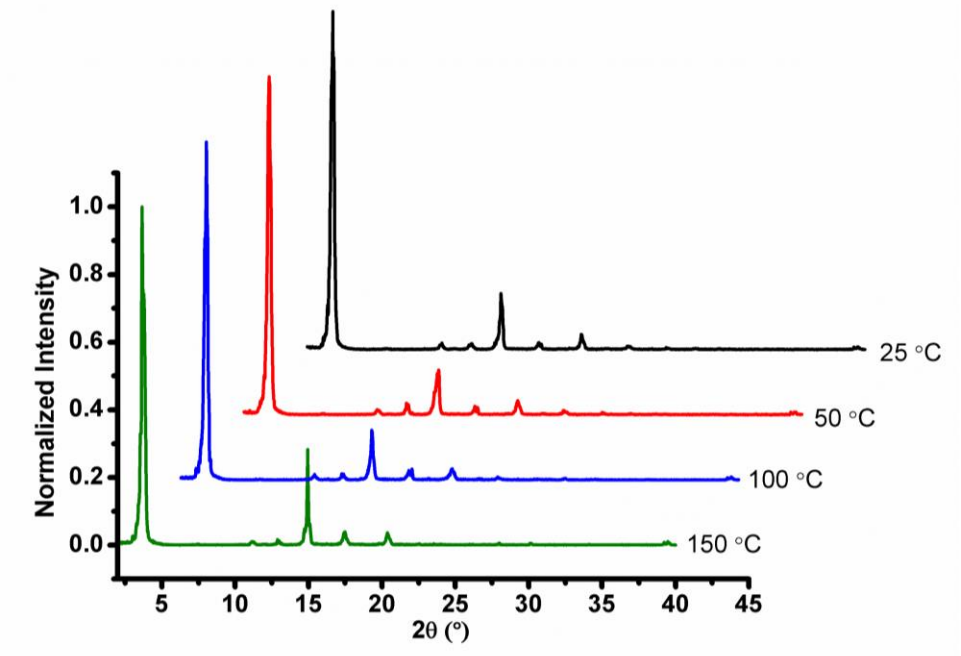

Figure S20. VTPXRD analysis of HxNDI

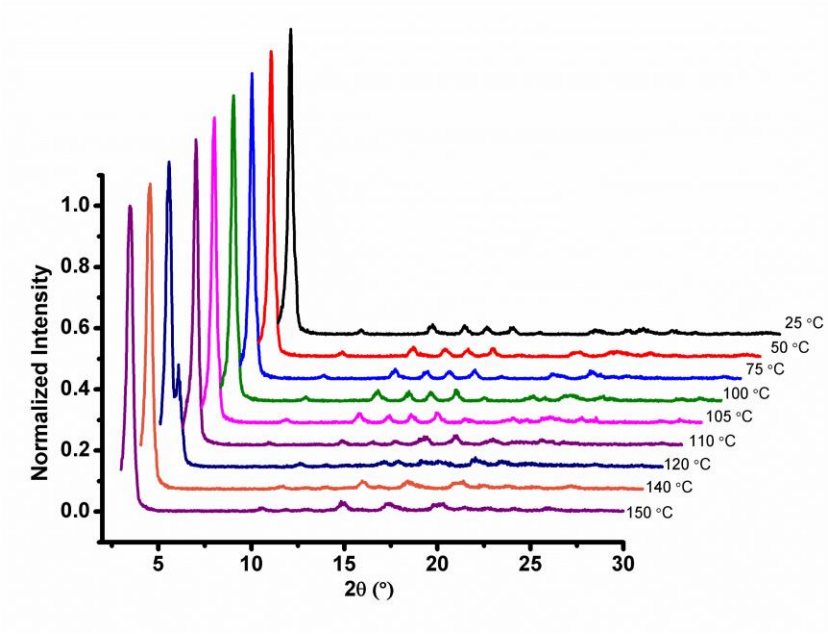

Figure S21. VTPXRD analysis of HNDI. Thermochromism occurs between 25 °C and 110 °C. At temperatures up to 110 °C, no significant changes were observed. Beyond 110 °C, changes to the 2θ values occurred due to changes in the crystalline phase.

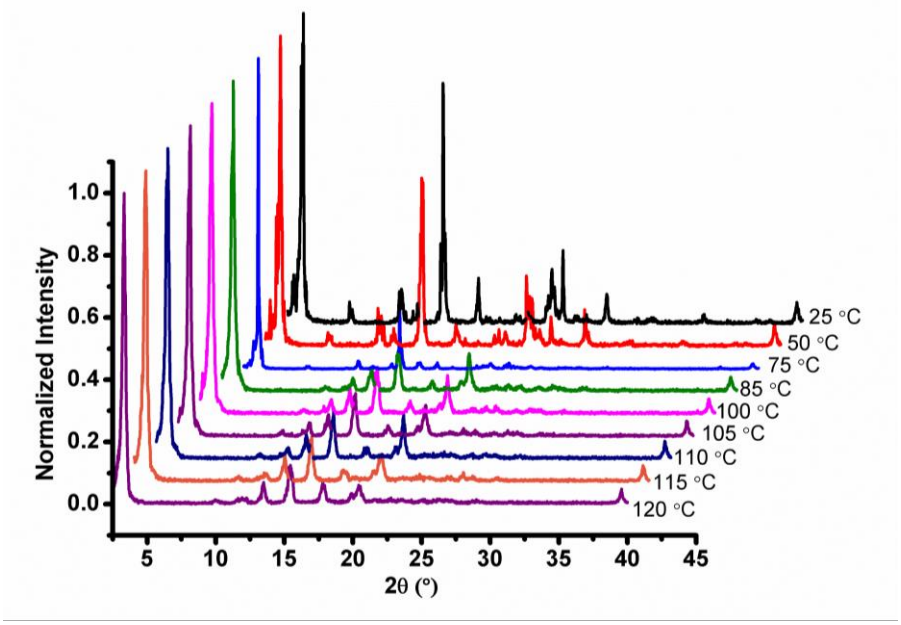

Figure S22. VTPXRD analysis of HNDI. Thermochromism occurs between 25 °C and 75 °C. At temperatures up to 75 °C, no significant changes were observed. Beyond 75 °C, changes to the 2θ values occurred due to changes in the crystalline phase.

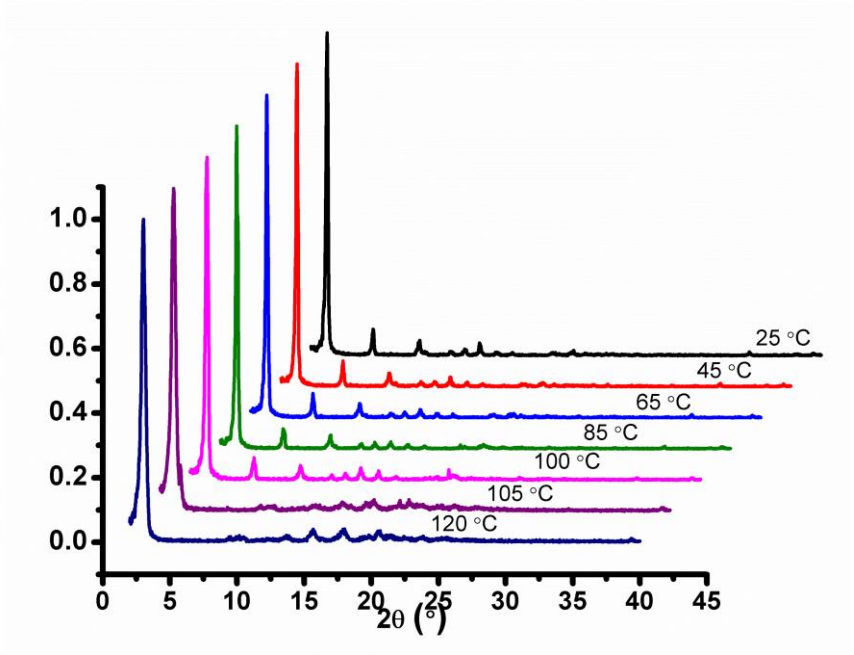

Figure S23. VTPXRD analysis of HNDI. Thermochromism occurs between 25 °C and 105 °C. At temperatures up to 105 °C, no significant changes were observed. Beyond 105 °C, changes to the 2θ values occurred due to changes in the crystalline phase.

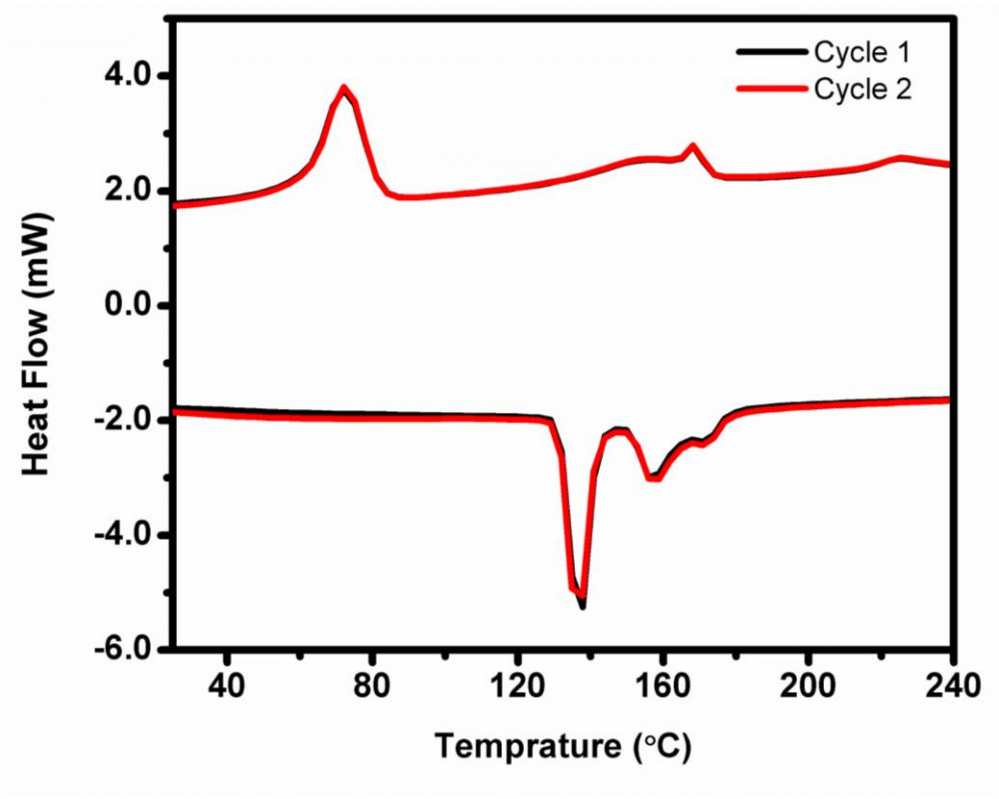

Figure S24. DSC curve for two consequent heating-cooling cycles of PNDI

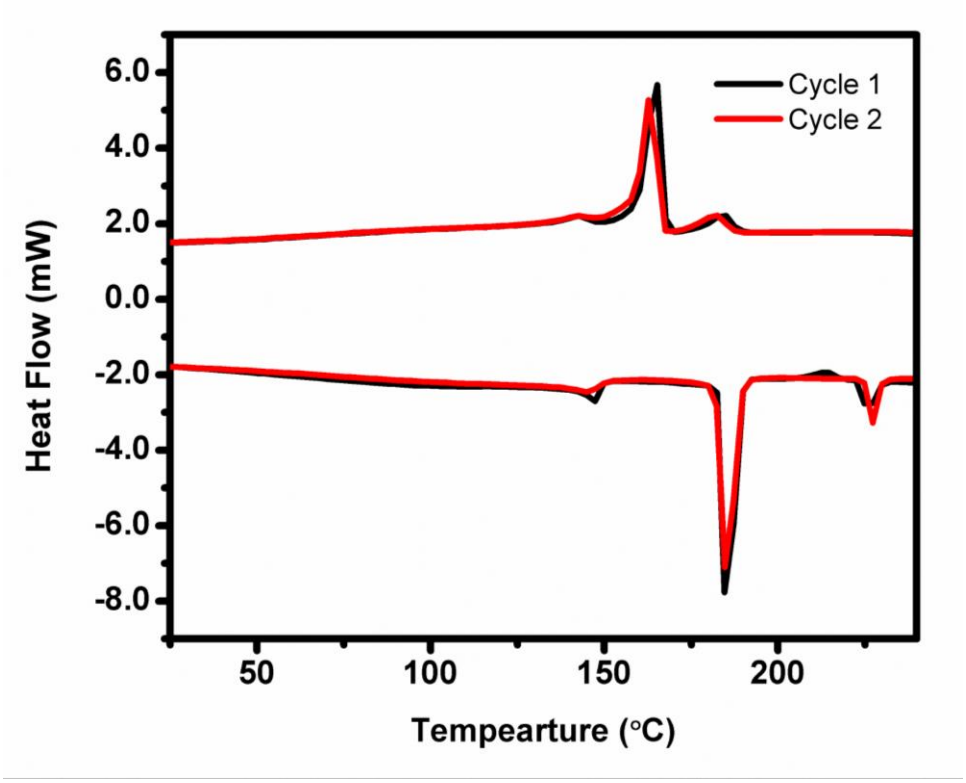

Figure S25. DSC curve for two consequent heating-cooling cycles of HxNDI

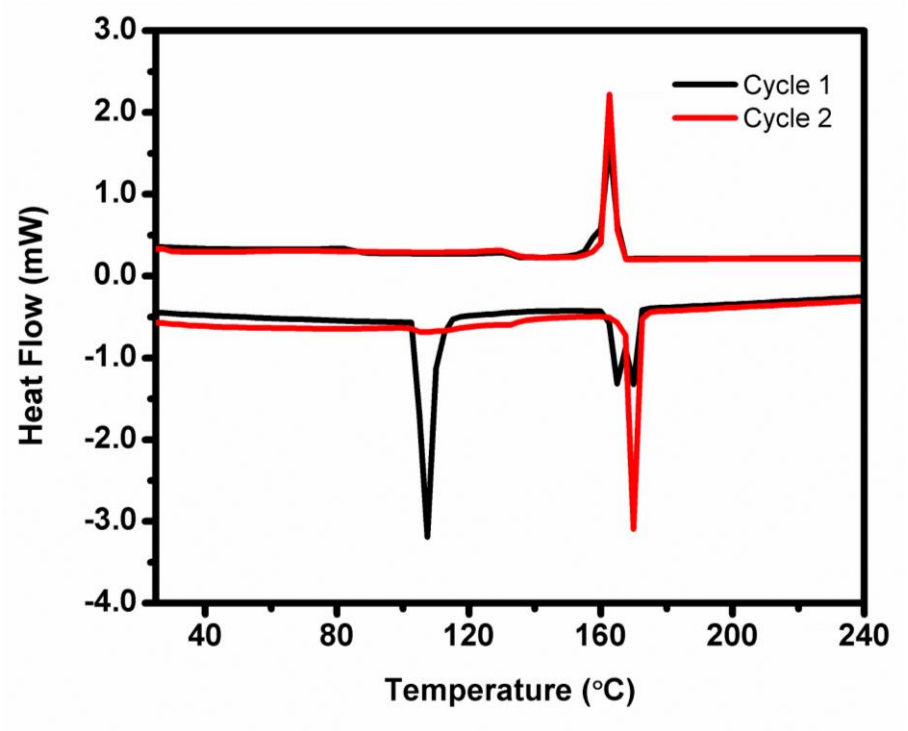

Figure S26. DSC curve for two consequent heating-cooling cycles of HxNDI

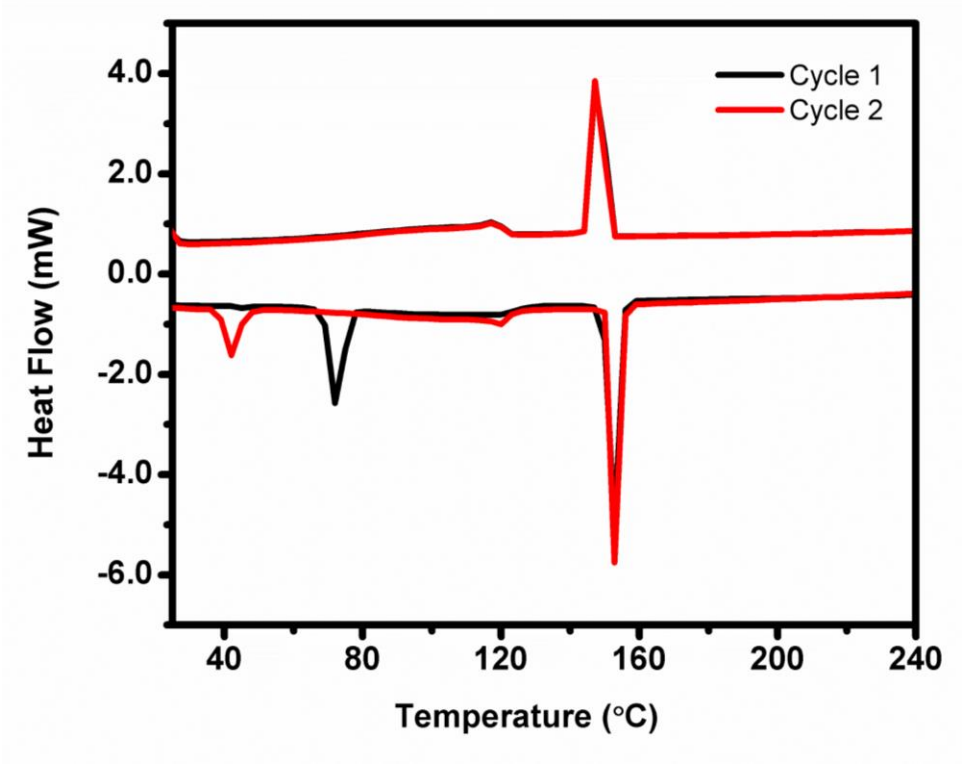

Figure S27. DSC curve for two consequent heating-cooling cycles of ONDI

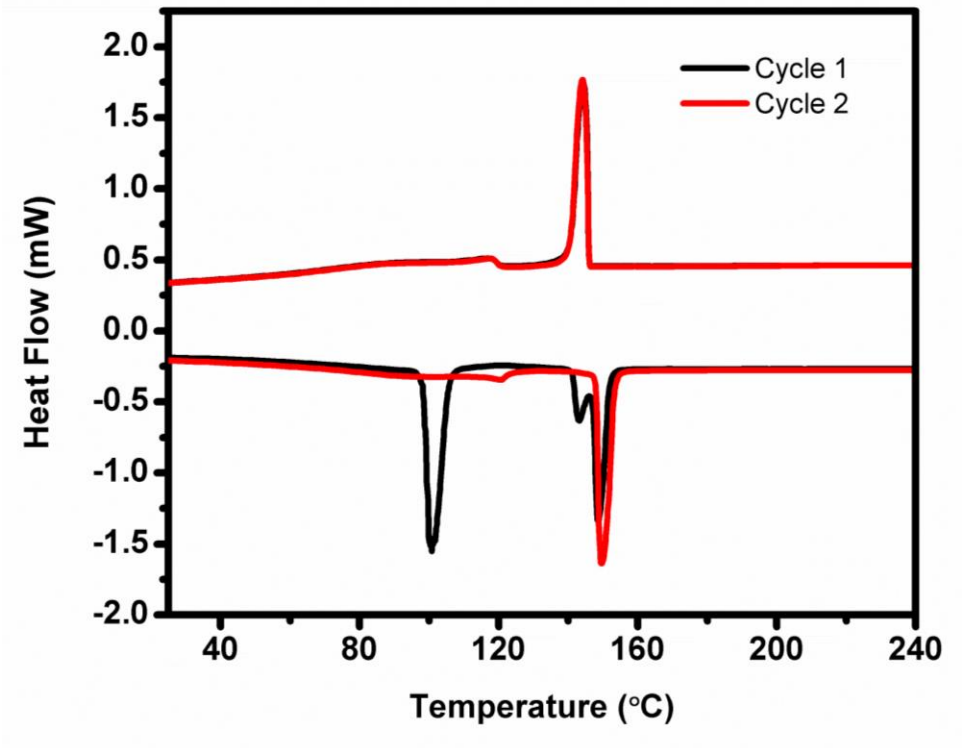

Figure S28. DSC curve for two consequent heating-cooling cycles of NNDI

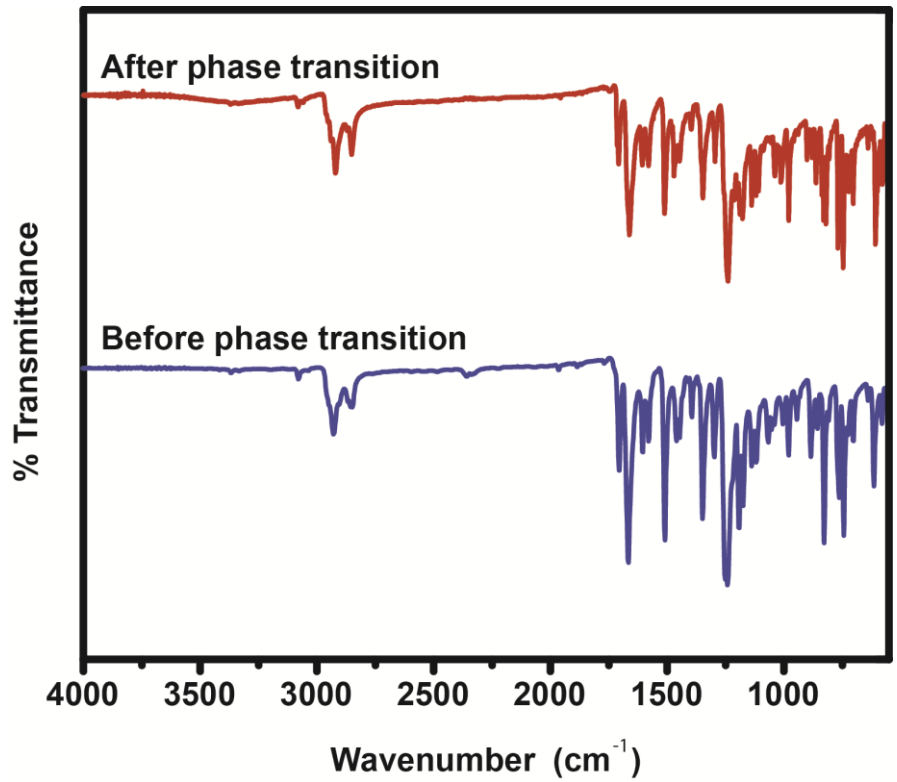

Figure S29. IR spectra of HNDI before and after irreversible phase transition

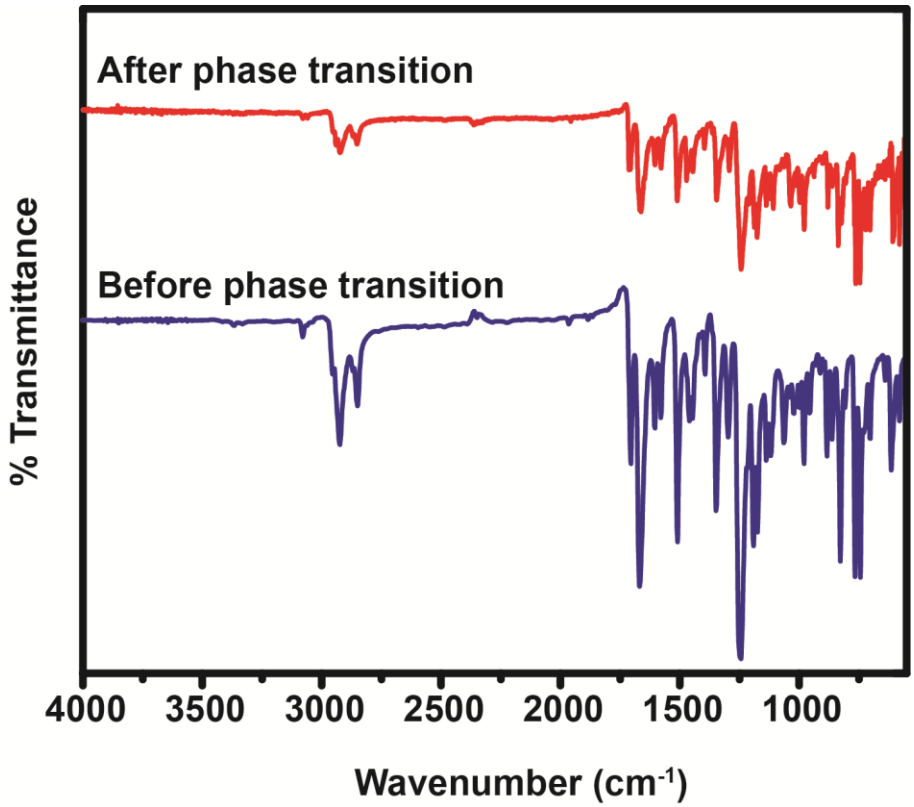

Figure S30. IR spectra of HNDI before and after irreversible phase transition

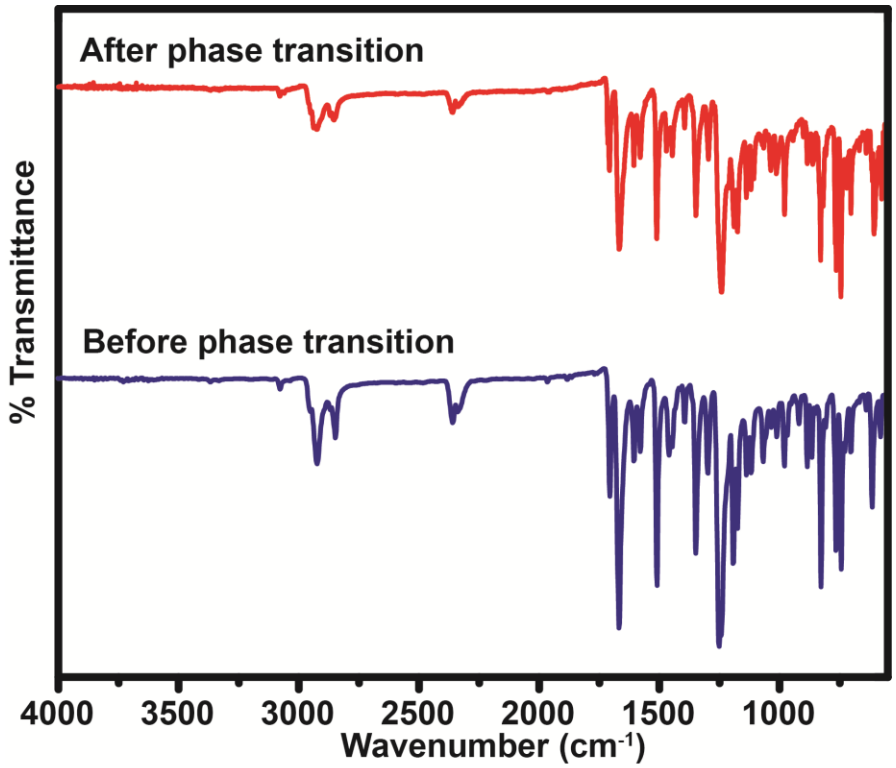

Figure S31. IR spectra of HNDI before and after irreversible phase transition

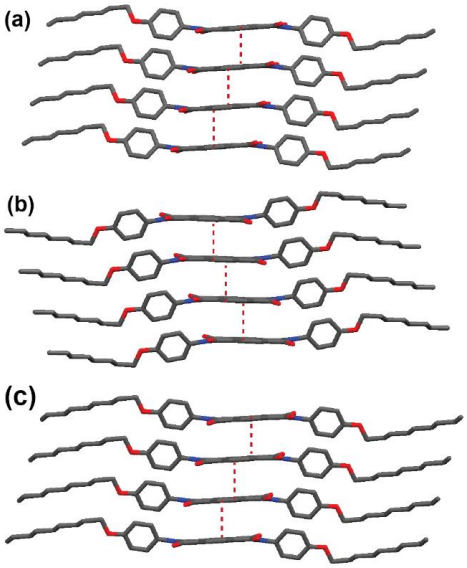

Figure S32. Comparison of interplanar distances of ANDI derivatives; (a) HNDI, (b) ONDI, and (c) NNDI.

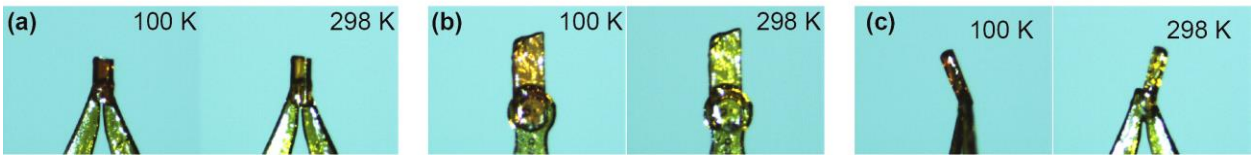

Figure S33. Thermochromism in the single crystals of (a) HNDI (b) ONDI and (c) NNDI

References

1. G. M. Sheldrick, *Acta Crystallogr., Sect. A: Found. Adv.*, 2015, **71**, 3-8.
2. G. M. Sheldrick, *Acta crystallographica. Section C, Structural chemistry*, 2015, **71**, 3-8.
3. M. Dharmarwardana, R. P. Welch, S. Kwon, V. K. Nguyen, G. T. McCandless, M. A. Omary and J. J. Gassensmith, *Chem. commun.*, 2017, **53**, 9890-9893.